Femtosecond streaking in ambient air

Korobenko, A.; Johnston, K.; Kubullek, M.; Arissian, L.; Dube, Z.; Wang, T.; Kübel, M.; Naumov, A. Yu.; Villeneuve, D. M.; Kling, M. F.; Corkum, P. B.; Staudte, A.; Bergues, B.

Publisher's version / Version de l'éditeur:
https://doi.org/10.1364/OPTICA.398846
Optica, 7, 10, pp. 1372-1376, 2020-10-08

optica

Femtosecond streaking in ambient air

A. Korobenko,[1,†] K. Johnston,[1,†] M. Kubullek,[4] L. Arissian,[1,2] Z. Dube,[1] T. Wang,[1] M. Kübel,[1,3] A. Yu. Naumov,[1] D. M. Villeneuve,[1] M. F. Kling,[4,5] P. B. Corkum,[1] A. Staudte,[1] and B. Bergues[1,4,5,*]

[1]Joint Attosecond Science Laboratory, National Research Council of Canada and University of Ottawa, Ottawa, Ontario K1A0R6, Canada
[2]National Research Council Canada, 100 Sussex Dr., Ottawa, Ontario K1A 0R6, Canada
[3]Institute for Optics and Quantum Electronics, University of Jena, Max-Wien-Platz 1, 07743 Jena, Germany
[4]Physics Department, Ludwig-Maximilians-Universität Munich, Am Coulombwall 1, 85748 Garching, Germany
[5]Max Planck Institute of Quantum Optics, Hans-Kopfermann-Straße 1, 85748 Garching, Germany
*Corresponding author: boris.bergues@mpq.mpg.de

Received 1 June 2020; revised 1 September 2020; accepted 1 September 2020 (Doc. ID 398846); published 8 October 2020

We demonstrate a novel method to measure the temporal electric field evolution of ultrashort laser pulses. Our technique is based on the detection of transient currents in air plasma. These directional currents result from subcycle ionization of air with a short pump pulse and the steering of the released electrons with the pulse to be sampled. We assess the validity of our approach by comparing it with different state-of-the-art laser-pulse characterization techniques. Notably, our method works in ambient air and facilitates a direct measurement of the field waveform, which can be viewed in real time on an oscilloscope in a similar way as a radio frequency signal.

https://doi.org/10.1364/OPTICA.398846

1. INTRODUCTION

The full characterization of coherent light fields is essential for both the understanding of light–matter interaction and its manipulation on time scales down to the period of a field oscillation. Many existing light-field characterization methods rely on the determination of the spectral amplitude and phase of the electric field [1]. While the measurement of the spectral amplitude is mostly trivial, the determination of the spectral phase is more challenging. This is the reason why most existing methods only provide partial phase information, typically leaving the carrier-envelope phase (CEP) undetermined [2–4] and thus preventing a complete characterization of the electric field.

An alternative approach to this problem is to measure the electric field in the time domain, as is done with an oscilloscope for electric fields up to gigahertz (GHz) frequencies. While field-sampling techniques based on Auston switches [5] or electro-optic sampling (EOS) [6] have allowed time-domain measurement of terahertz (THz) waves, transposing these techniques into the optical frequency range has long remained a serious challenge. The latter was finally met two decades ago, owing to the development of laser sources for near single-cycle pulses [7,8] and the introduction of the attosecond streaking technique [9,10].

Attosecond streaking relies on the generation of gas-phase high-harmonic generation (HHG) of the infrared (IR) waveform to be sampled, referred to as the streaking pulse in the following. For a near singe-cycle IR pulse with the right carrier-envelope phase, HHG gives rise to a single attosecond burst of extreme ultraviolet (XUV) radiation. This XUV pulse, which acts as a gate, is much shorter than the period of the fundamental. After introducing a variable delay between the gating and streaking pulses, both pulses are focused onto a gas target.

Photoelectrons generated upon XUV ionization of the atoms by the gating pulse are accelerated by the streaking field. This results in the so-called ponderomotive streaking, i.e., a shift Δp_e of the final electron momentum p_e that is proportional to the vector potential $A(t_i)$ of the streaking pulse at the instant t_i of ionization [11]. The temporal evolution of the IR field is inferred from the delay-dependent electron momentum usually measured with an electron time-of-flight spectrometer. While it is a powerful technique to time resolve XUV–matter interactions, the original attosecond streaking requires a complex high-vacuum setup and a time-of-flight spectrometer.

Several techniques enabling a full characterization of laser pulses have been developed since then. Like attosecond streaking, the majority of these field-sampling techniques rely on the use of a short auxiliary pulse providing a subcycle nonlinear gating [12–17]. In the time-domain observation of an electric field (TIPTOE) approach [13], a strong few-cycle phase-stable gating pulse tunnel ionizes a target gas, while the ionization rate is modulated by the much weaker field to be sampled. This modulation can be measured electronically [13] or optically [14]. More recently, the streaking technique was adapted to sample infrared laser fields with a few-cycle visible pulses via ionization of a dilute gas target [18] or via electron–hole pair excitation in solid crystals [16].

Here we introduce a novel technique facilitating streaking in ambient air, i.e., the direct measurement of the light field under

ambient conditions. Our approach relies on the measurement of transient currents in ambient-air plasma, recently demonstrated by Kubullek *et al.* [19], and it leads to an order-of-magnitude simpler implementation of the streaking concept. In particular, we anticipate that our technique will become an attractive tool for the characterization of infrared and mid-infrared pulses generated in novel state-of-the-art laser systems.

2. EXPERIMENTAL SETUP

In our proof-of-principle experiment, we use a few-cycle 800 nm pulse with nonstabilized CEP as a gating pulse to sample a CEP-stable streaking field with a central wavelength at around 2.2 μm.

Both the streaking field and the gating pulse are generated from Coherent Legend Cryo-HE 10 kHz Ti:Sa laser system delivering 1.3 mJ pulses with a duration of 25 fs full width at half-maximum (FWHM) and a central wavelength of 800 nm.

The experimental setup is presented in Fig. 1(a). Around 90% of the output power is used to pump Light Conversion TOPAS-Prime optical parametric amplifier (OPA) producing phase-stable idler streaking pulses with a central wavelength tunable in a spectral range from 1.8 to 2.4 μm. In order to generate the gating pulses, 10% of the beam power is split off with a dielectric beam splitter and spectrally broadened inside an Ar-filled hollow-core fiber (HCF). The resulting pulses with a central wavelength at 770 nm are sent through a chirped mirror compressor, a 3 mm thick KD_2PO_4 (KDP) crystal and a pair of fused silica wedges, where they are recompressed to a FWHM duration of 5 fs.

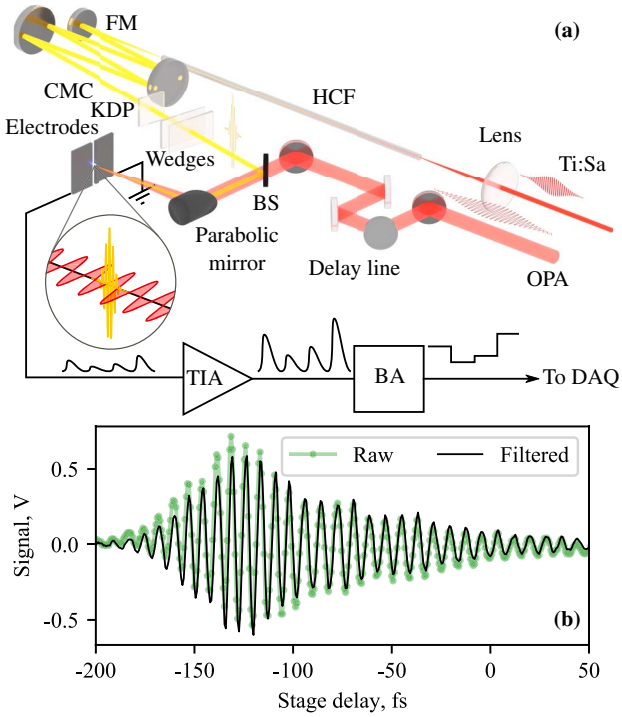

Fig. 1. **(a)** Experimental setup. An output of a Ti:sapphire laser (Ti:Sa) is passed through an Ar-filled hollow-core fiber (HCF), recollimated with a silver focussing mirror (FM), and compressed in a chirped-mirror compressor (CMC). It is combined with an idler of an OPA on a silicon beam splitter (BS) and focused by an off-axis parabolic mirror in between a pair of metal electrodes. The current, picked up by electrodes, is amplified in a transimpedance amplifier (TIA), followed by a boxcar averager (BA). Finally, the signal is read by a computer via a data acquisition card (DAQ). **(b)** Sample delay scan of the signal. Green dots are raw data, black line is the data after applying a band-pass filter. See text for details.

The vertically polarized gating pulse (Ti:Sa) and the horizontally polarized streaking pulse (OPA) are attenuated using neutral density filters to 20 μJ and 30 μJ, respectively. The two beams are then combined on a silicon beam splitter (BS) positioned at Brewster's angle for the streaking pulse in order to minimize the reflection losses. A 90° off-axis parabolic silver mirror with an effective focal length of 150 mm is used to focus the collinear streaking and gating beams into ambient air down to FWHM spot sizes of 35 μm and 30 μm and peak intensities of 4×10^{13} W/cm^2 and 1×10^{14} W/cm^2, respectively. The gating pulse intensity is high enough to tunnel ionize air and generate a narrow plasma channel with a width of 13 μm and a length of 190 μm FWHM. Since the length of the plasma channel is much shorter than the 1.6 mm Rayleigh range of the streaking pulse, the Gouy phase shift has no effect in our measurements. The transient polarization induced in the air plasma is probed by measuring the current flowing through a pair of plane-parallel electrodes placed on either side of the plasma channel. The electrodes are made of 500 μm thick aluminum plates extending over the whole length of the plasma channel to maximize the signal coupling of the induced currents. Separated by a 140 μm wide gap, they allow both beams to go through without clipping. While it simplifies the alignment, increasing the separation between the electrodes results in a decrease of the signal. We attribute this to the reduced capacitive coupling as discussed later in the text. We orient the electrodes perpendicularly to the polarization of the streaking pulse. To increase the stability of the measurement, we mount all optical components on a single massive optical table, equipped with covers to lessen the effect of airflow.

The current is amplified in a transimpedance amplifier (TIA) and integrated over a time window of 30 μs using a boxcar averager (BA) voltage amplifier. The amplification factors of the TIA and BA are 1 V/1 μA and 1 V/5 mV, respectively. The boxcar DC voltage output, which is proportional to the charges flowing in the circuit, is recorded with a computer via a data acquisition card (DAQ). In the streaking beam path, a delay stage driven with a precision piezo positioner permits control of the delay between gating and streaking pulses with subfemtosecond precision.

Two different modes, a fast and a slow mode, can be employed to scan the delay. In the fast mode, the stage is moving at a constant speed of 0.5 mm/s throughout the desired scanning range, while the signal is acquired continuously with the DAQ. This mode allowed to scan a picosecond range within a few hundreds of milliseconds, facilitating real-time observation of the measured waveforms on an oscilloscope at 2 Hz refresh rate. Although useful for a quick estimate of the waveform during alignment, we found that measurements using this fast mode were flawed due to an uneven motion of the piezo stage at higher speed. For the sake of accuracy, all data presented in the following were acquired in the slow mode, where the delay stage was moved in discrete steps of 100 nm (0.67 fs) and the DAQ input was averaged over 200 laser shots after each step, stretching a single scan to around 2 min. The resulting delay-dependent signal is plotted in Fig. 1(b). In order to clean the raw signal (green dots) from parasitic noise, we numerically apply a band-pass filter with a high- and low-frequency cutoff corresponding to wavelengths of 0.5 μm and 4 μm, respectively. This leaves only physically relevant optical frequencies, resulting in the waveform, shown with a solid black line in Fig. 1(b).

An alternative characterization of the streaking field is performed with a second-harmonic-generation frequency-resolved optical gating (SHG FROG) [2] and a streak camera for strong-field ionization (STIER) [18]. For the STIER measurement, half of the combined beam is picked off by a D-shaped pick-off mirror and redirected into a standard cold target recoil-ion momentum spectroscopy (COLTRIMS) apparatus, while the other half of the beam continues to the air-streaking setup.

A detailed description of the STIER technique can be found in Ref. [18]. Briefly, inside the COLTRIMS vacuum chamber, the beams are focused onto a supersonic D_2 molecular gas jet with a parabolic mirror. The electrons and ions generated in the interaction region are guided by homogeneous and parallel electric and magnetic fields onto two time- and position-sensitive detectors. The three-dimensional ion momentum reconstructed from the time and position information is measured as a function of the delay between the pulses. As demonstrated in Ref. [18], the delay-dependent D_2^+ momentum is proportional to the vector potential of the streaking field.

3. RESULTS AND DISCUSSION

The measured streaking signal is shown in Fig. 2(a), where the filtered waveform obtained from single scans (grey lines) is plotted together with an average over 10 scans (red line). We observe a slight variation (with a 2 fs RMS) in the offset delay of consecutive scans. This offset was compensated by shifting the waveforms of the individual scans along the delay axis to maximize their overlap prior to averaging. The agreement between the single and the averaged waveforms demonstrates the reproducibility of the measurement up to this small random delay offset. The ~7 fs period of the observed oscillation is in agreement with the 2.2 μm central wavelength of the streaking field.

In the following, we will show how the measured signal relates to the electromagnetic field of the streaking pulse. To this end, we first compare in Fig. 2(b) the power spectrum calculated from the measured traces (solid line) with that of the streaking pulse measured with an IR spectrometer (dashed line). For the latter, we verified that the propagation through the ionization volume did not significantly perturb the streaking pulse by measuring the spectra both before and after the focus. In Fig. 2(c) we show the result of the same comparison for different OPA output pulses with central wavelengths ranging from 1.9 to 2.25 μm. The wavelength dependence of the air-streaking and spectrometer measurements follows the same trend. We attribute the discrepancies observed at shorter wavelengths to a jitter in the pulse delay that is inherent to our setup and predominantly affects higher frequencies.

Applying the Yudin–Ivanov tunneling rate [20] for the ionization of air molecules by our gating pulse, we estimate that the FWHM of the CEP-averaged gate amounts to 2.6 fs FWHM. We calculate the spectral sensitivity as the Fourier spectrum of the gating window and find that the spectral sensitivity drops by a factor of two at a wavelength of 1.7 μm compared to its value in the long-wavelength limit. In practice, additional delay jitter could further limit the spectral sensitivity. Using a CEP-stabilized source, the ionization can be confined to less than a single half-cycle of the gating pulse, reaching gating window widths between 400 and 500 as, depending on the peak intensity [13]. This suggests that, with CEP stable pulses and an improved interferometer stability, our method should also be applicable to the sampling of visible pulses [21], with gating widths similar to those achieved in Refs. [13,14].

In general, even small noise in the time domain can result in strong variation of the spectral characteristics. In Fig. 3, the temporal amplitude and phase of the streaking pulse reconstructed from an independent SHG FROG measurement (dashed orange and blue lines, respectively) are compared to the amplitude and phase extracted from the air-streaking measurement (solid orange and blue lines, respectively). The CEP left undetermined in the FROG measurement was adjusted to maximize the agreement between both curves. As can be deduced from the similarity of the temporal

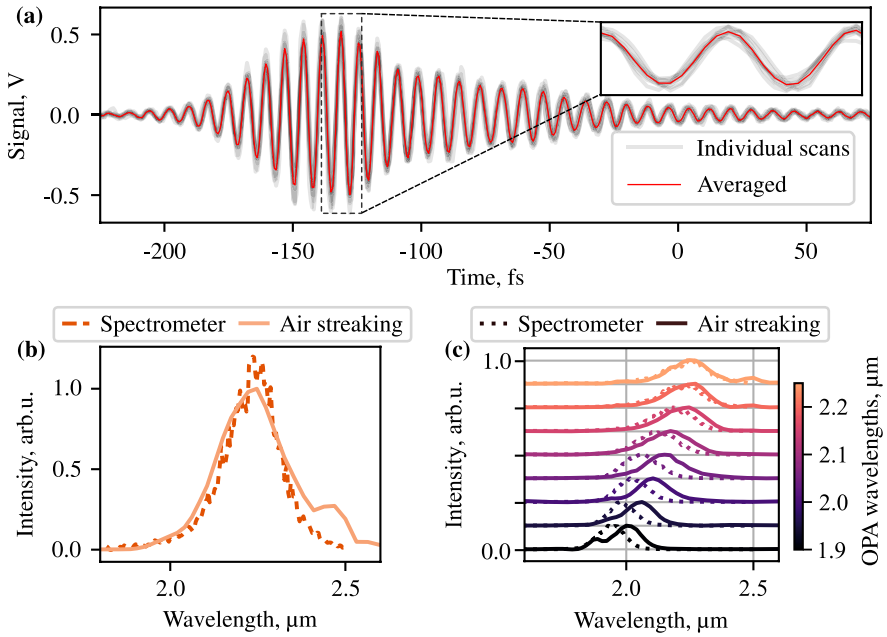

Fig. 2. **(a)** Individual filtered air-streaking scans (grey) and their average (red). A magnified region containing just two laser periods is shown in the inset. **(b)** Spectral intensity of the averaged air-streaking trace (solid line) and the spectrum measured with an IR spectrometer (dashed line). **(c)** Air-streaking (solid lines) and spectrometer (dashed lines) measurements of OPA pulses with different wavelengths, illustrated by the color code.

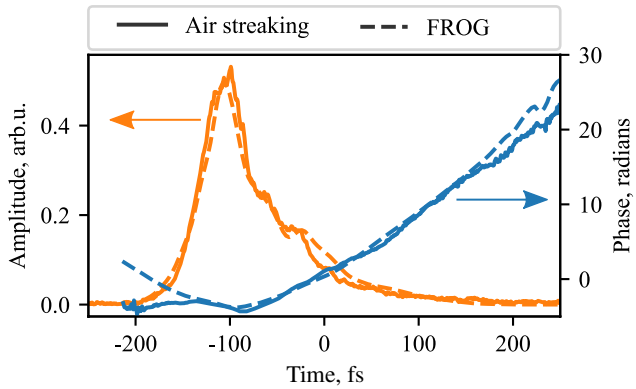

Fig. 3. Comparison between the temporal amplitudes (orange) and phases (blue), retrieved with air streaking (solid lines) and SHG FROG (dashed lines).

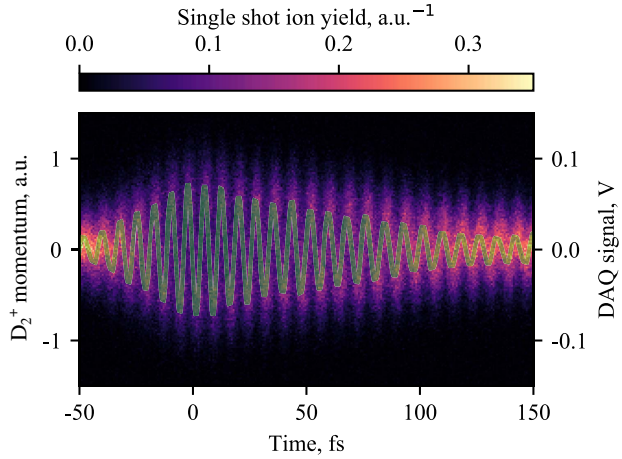

Fig. 4. Distribution of the z component of the D_2^+ recoil momentum, measured with the STIER technique (color map) and the waveform retrieved from ambient-air streaking (green line). The air-streaking waveform was propagated numerically to account for the optical path difference in the two measurements. The line thickness represents the experimental error.

amplitude and phase obtained with both methods, ambient-air streaking and FROG lead to comparable results.

Despite the good agreement between the two measurements, the ambiguity in the CEP inherent to the FROG technique prohibits a definite statement about the exact nature of the air-streaking signal. In regard to the complex collective electron dynamics in the plasma, it is *a priori* not clear how the phase of the measured current relates to that of the driving field. As argued in Ref. [22], electron scattering with neighboring atoms and ions in ambient-air plasma may significantly impact the induced transient current, and one may thus expect a possible effect on its phase. Other studies, in contrast, suggest that the induced current is in phase with the vector potential of the field [23]. In order to shed more light onto the nature of the measured air-streaking signal, we performed a parallel measurement of the waveform with the STIER method [18]. The comparison of the two experiments is especially interesting, as STIER is a streaking measurement on a single molecule and as such provides a clean reference. To account for the slight differences in dispersion along the path from the pick-off mirror to the respective interaction regions in both measurements, the waveform retrieved from the air-streaking measurement was propagated numerically through the extra air in the STIER arm. Additional mirror reflections were also taken into account.

The recorded delay-dependent distribution of the ion momentum along the IR polarization axis is shown in Fig. 4 together with the numerically propagated air-streaking signal. We find that both signals oscillate essentially in phase, with the ion signal slightly lagging behind by $\Delta\varphi = (500 \pm 700)$ mrad. The error mostly results from the uncertainty in propagation lengths in air and optical windows. This finding suggests that ambient-air streaking samples the vector potential. Further studies are needed, however, to confirm and fully elucidate the mechanism that governs the transient current generation [21].

While we found that, for the purpose of pulse characterization, perpendicular polarization of the gating and streaking pulses corresponds, indeed, to the optimum configuration, it was demonstrated in Ref. [18] using STIER that for collinearly polarized gating and streaking pulses, the IR affects both the ionization yield and the electron deflection, providing insights into the dynamics of tunnel ionization.

It is instructive to compare the present method to the related TIPTOE technique [13]. Similar to air streaking, it probes a current flowing between metal electrodes in ambient air to sample the light waveform. Despite these similarities, there are, however, important differences between the two.

One of them concerns the current detection. As shown in Ref. [13], provided the bias DC field applied in TIPTOE to separate electrons and ions is strong enough, the electrons cross the large air gap and eventually make their way to the electrodes. On the other hand, in the recently reported single-shot CEP measurements in ambient air [19] or optoelectronic field measurement in solids [16], the separated charges recombine before reaching the electrodes, so the measured current is a displacement current.

In ambient-air streaking, where no external field is applied, the electron motion is essentially determined by the vector potential of the streaking field. As such, at a typical electron momentum transfer cross section of 10^{-15} cm^2 [24] in air, the induced current is expected to decay after only $\lambda \sim 1/(2.5 \times 10^{19}\ \mathrm{cm}^{-3} \cdot 10^{-15}\ \mathrm{cm}^2) = 400$ nm of propagation, i.e., a few orders of magnitude less than the electrode separation. This suggests that the current measured in ambient-air streaking is also a displacement current. The practical implication of detecting a displacement current rather than charges reaching the electrodes is yet to be determined. While a possible disadvantage may be a reduced sensitivity as compared to the charge detection, the lower requirements to the conductive properties of the electrode surface may represent an asset.

In TIPTOE, the tunnel ionization yield from the gating pulse is modulated by the electric field to be sampled. Since the sign of the gating field changes every half cycle, it is important to concentrate the plasma production to essentially a single half-cycle. As a consequence, the gating pulse must be CEP stabilized with a duration close to a single cycle. Even then, a separate measurement is required to determine the absolute direction of the electric field. This is in contrast to the present method, which does not require a CEP-stable gating pulse and yet allows for the determination of the CEP of the streaking pulse.

4. CONCLUSION

In conclusion, we have introduced air streaking as a novel technique to measure the electromagnetic field of a coherent light wave. While similar to attosecond streaking, our technique avoids the HHG step and works in ambient air, providing a direct measurement of the vector potential. The measured field can be viewed in real time on any standard oscilloscope in the same way as a radio frequency electronic signal. The potential of the technique reaches far beyond waveform characterization applications. In a similar way that attosecond and solid-state streaking have permitted time resolution of XUV–matter interactions and carrier dynamics in crystals, respectively, ambient-air streaking opens the door for the study of time-domain subfemtosecond dynamics inside plasmas.

Funding. Air Force Office of Scientific Research (FA9550-16-1-0109); Canada Research Chairs; Natural Sciences and Engineering Research Council of Canada; Joint Center for Extreme Photonics; Deutsche Forschungsgemeinschaft (KL-1439/11-1, LMUexcellent); Max-Planck-Gesellschaft; European Research Council (FETopen PetaCOM).

Acknowledgment. We thank David Crane and Ryan Kroeker for their technical support, and we are grateful for fruitful discussions with Marco Taucer, Guilmot Ernotte, Dmitry Zimin, Nicholas Karpowicz, and Shawn Sederberg.

Disclosures. The authors declare no conflicts of interest.

[†]These authors contributed equally to this paper.

REFERENCES

1. R. Trebino, *Frequency-Resolved Optical Gating: The Measurement of Ultrashort Laser Pulses* (Springer, 2000).
2. D. J. Kane and R. Trebino, "Characterization of arbitrary femtosecond pulses using frequency-resolved optical gating," IEEE J. Quantum Electron. **29**, 571–579 (1993).
3. C. Iaconis and I. A. Walmsley, "Self-referencing spectral interferometry for measuring ultrashort optical pulses," IEEE J. Quantum Electron. **35**, 501–509 (1999).
4. M. Miranda, T. Fordell, C. Arnold, A. L'Huillier, and H. Crespo, "Simultaneous compression and characterization of ultrashort laser pulses using chirped mirrors and glass wedges," Opt. Express **20**, 688–697 (2012).
5. D. H. Auston, K. P. Cheung, and P. R. Smith, "Picosecond photoconducting Hertzian dipoles," Appl. Phys. Lett. **45**, 284–286 (1984).
6. Q. Wu and X. C. Zhang, "Ultrafast electro-optic field sensors," Appl. Phys. Lett. **68**, 1604–1606 (1996).
7. E. Goulielmakis, "Direct measurement of light waves," Science **305**, 1267–1269 (2004).
8. Y. Mairesse, O. Gobert, P. Breger, H. Merdji, P. Meynadier, P. Monchicourt, M. Perdrix, P. Salières, and B. Carré, "High harmonic XUV spectral phase interferometry for direct electric-field reconstruction," Phys. Rev. Lett. **94**, 173903 (2005).
9. J. Itatani, F. Quéré, G. L. Yudin, M. Y. Ivanov, F. Krausz, and P. B. Corkum, "Attosecond streak camera," Phys. Rev. Lett. **88**, 173903 (2002).
10. R. Kienberger, E. Goulielmakis, M. Uiberacker, A. Baltuska, V. Yakovlev, F. Bammer, A. Scrinzi, T. Westerwalbesloh, U. Kleineberg, U. Heinzmann, M. Drescher, and F. Krausz, "Atomic transient recorder," Nature **427**, 817–821 (2004).
11. U. Thumm, Q. Liao, E. M. Bothschafter, F. Süßmann, M. F. Kling, and R. Kienberger, "Attosecond physics: attosecond streaking spectroscopy of atoms and solids," in *Fundamentals of Photonics and Physics* (Wiley, 2015), Chap. **13**, pp. 387–441.
12. K. T. Kim, C. Zhang, A. D. Shiner, B. E. Schmidt, F. Légaré, D. M. Villeneuve, and P. B. Corkum, "Petahertz optical oscilloscope," Nat. Photonics **7**, 958–962 (2013).
13. S. B. Park, K. Kim, W. Cho, S. I. Hwang, I. Ivanov, C. H. Nam, and K. T. Kim, "Direct sampling of a light wave in air," Optica **5**, 402–408 (2018).
14. N. Saito, N. Ishii, T. Kanai, and J. Itatani, "All-optical characterization of the two-dimensional waveform and the Gouy phase of an infrared pulse based on plasma fluorescence of gas," Opt. Express **26**, 24591–24601 (2018).
15. S. Keiber, S. Sederberg, A. Schwarz, M. Trubetskov, V. Pervak, F. Krausz, and N. Karpowicz, "Electro-optic sampling of near-infrared waveforms," Nat. Photonics **10**, 159–162 (2016).
16. S. Sederberg, D. Zimin, S. Keiber, F. Siegrist, M. S. Wismer, V. S. Yakovlev, I. Floss, C. Lemell, J. Burgdörfer, M. Schultze, F. Krausz, and N. Karpowicz, "Attosecond optoelectronic field measurement in solids," Nat. Commun. **11**, 430 (2020).
17. T. Hammond, A. Korobenko, A. Y. Naumov, D. M. Villeneuve, P. B. Corkum, and D. H. Ko, "Near-field imaging for single-shot waveform measurements," J. Phys. B **51**, 065603 (2018).
18. M. Kübel, Z. Dube, A. Y. Naumov, M. Spanner, G. G. Paulus, M. F. Kling, D. M. Villeneuve, P. B. Corkum, and A. Staudte, "Streak camera for strong-field ionization," Phys. Rev. Lett. **119**, 183201 (2017).
19. M. Kubullek, Z. Wang, K. von der Brelje, D. Zimin, P. Rosenberger, J. Schötz, M. Neuhaus, S. Sederberg, A. Staudte, N. Karpowicz, M. F. Kling, and B. Bergues, "Single-shot carrier–envelope-phase measurement in ambient air," Optica **7**, 35–39 (2020).
20. G. L. Yudin and M. Y. Ivanov, "Nonadiabatic tunnel ionization: looking inside a laser cycle," Phys. Rev. A **64**, 013409 (2001).
21. D. Zimin, M. Weidman, J. Schoetz, M. F. Kling, V. Yakovlev, F. Krausz, and N. Karpowicz are preparing a manuscript to be called "Nonlinear photoconductive sampling at optical frequencies in air."
22. M. Kreß, T. Löffler, M. D. Thomson, R. Dörner, H. Gimpel, K. Zrost, T. Ergler, R. Moshammer, U. Morgner, J. Ullrich, and H. G. Roskos, "Determination of the carrier-envelope phase of few-cycle laser pulses with terahertz-emission spectroscopy," Nat. Phys. **2**, 327–331 (2006).
23. K.-Y. Kim, J. H. Glownia, A. J. Taylor, and G. Rodriguez, "Terahertz emission from ultrafast ionizing air in symmetry-broken laser fields," Opt. Express **15**, 4577–4584 (2007).
24. A. G. Engelhardt, A. V. Phelps, and C. G. Risk, "Determination of momentum transfer and inelastic collision cross sections for electrons in nitrogen using transport coefficients," Phys. Rev. **135**, A1566–A1574 (1964).